Classical Analogs for Electromagnetically Induced Transparency

Joshua Zadoyko

Department of Physics and Electrical Engineering, University of Scranton

Thursday, May 10th, 2018

Objective

- Understand the fundamental concepts of a quantum process known as electromagnetically induced transparency (EIT)
- Model EIT classically as spring-mass system and coupled RLC circuit
- Compare the classical models to the quantum system
- Observe EIT-like behavior experimentally in a coupled RLC circuit

Fundamental concepts of EIT

- EIT is a technique for eliminating the effect a medium has on a propagating beam of light

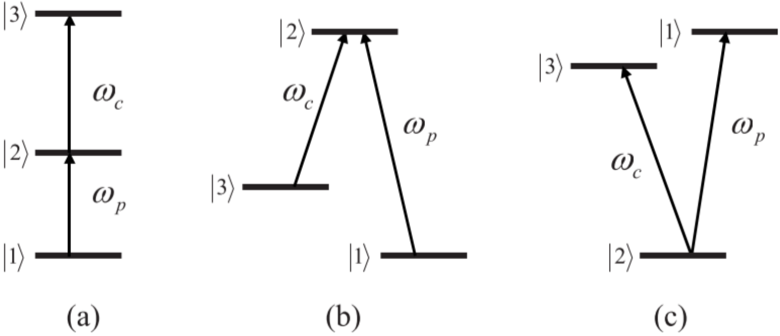

Figure 1: (a) ladder-type (b) lambda-type (c) V-type. The levels $|1\rangle$ and $|2\rangle$ are coupled by the probe field with frequency ω_p, and levels $|2\rangle$ and $|3\rangle$ are coupled by the coupling field with frequency ω_c.

Fundamental concepts of EIT

$$P = P_0 + \epsilon_0 \chi_e E + \epsilon_0 \chi_e E^2 + \ldots$$
$$\chi_e = \chi^{(1)} + i\chi^{(2)}$$

- The zero absorption window is described by the imaginary part of complex electric susceptibility $\chi^{(2)}$

$$\alpha = \frac{\omega_p n_0 \chi^{(2)}}{c}$$

- The index of refraction is described by the imaginary part of the complex electric susceptibility $\chi^{(1)}$

$$\beta = \frac{\omega_p n_0 \chi^{(1)}}{2c}$$

Semi-classical analysis of EIT

- diagonal elements give the probability that the system is in energy eigenstate n
- off-diagonal element describe the coherence between levels *n* and *m*

$$\dot{\rho}_{nm} = -\frac{i}{\hbar}[\hat{H}, \hat{\rho}]_{nm} - \gamma_{nm}(\rho_{nm} - \rho_{nm}^{eq}).$$

- phenomenological damping term, indicating that ρ_{nm} relaxes to its equilibrium value ρ_{nm}^{eq} at its decay rate γ_{nm}

$$H = \frac{\hbar}{2}\begin{bmatrix} 0 & \Omega_p & 0 \\ \Omega_p & -2\Delta_p & \Omega_c \\ 0 & \Omega_c & -2(\Delta_p - \Delta_c) \end{bmatrix}$$

Resulting density matrix equations

$$
\begin{aligned}
\dot{\rho}_{21} =& i g_{21} E_p(\rho_{22} - \rho_{11}) + (i\Delta_p - \gamma_{21})\rho_{21} - i g_{32} E_c \rho_{32}, \\
\dot{\rho}_{31} =& i g_{21} E_p \rho_{32} + [i(\Delta_p - \Delta_c) - \gamma_{31}]\rho_{31} - i g_{32} E_c \rho_{21}, \\
\dot{\rho}_{32} =& i g_{21} E_p \rho_{31} - (i\Delta_c + \gamma_{32})\rho_{32} - i g_{32} E_c(\rho_{22} - \rho_{33}).
\end{aligned}
$$

- The resulting density matrix elements can be found by solving the differential systems of equations above as

$$
\begin{aligned}
\rho_{21} &= \frac{-i g_{21} E_p e^{-i\omega_p t}}{(\gamma_{21} - i\Delta_p) + \frac{\Omega_c^2/4}{\gamma_{31} - i(\Delta_p + \Delta_c)}}, \\
\rho_{31} &= \frac{-i g_{32} E_c e^{-i\omega_c t}}{\gamma_{31} - i(\Delta_p - \Delta_c)}\rho_{21}.
\end{aligned}
$$

Polarization and the density matrix elements

- The relationship between the first order complex susceptibility and the polarization and the atomic polarization per unit volume

$$P = \frac{1}{2}\epsilon_0 E_p[\chi_e e^{-i\omega_p t} + c.c]$$

$$P = -2\hbar g_{21} N \rho_{21} + c.c$$

$$\chi_e = \frac{4i\hbar g_{21}^2/\epsilon_0}{(\gamma_{21} - i\Delta_p) + \frac{\Omega_c^2/4}{\gamma_{31} - i(\Delta_p + \Delta_c)}}$$

Theoretical results demonstrating EIT in rubidium

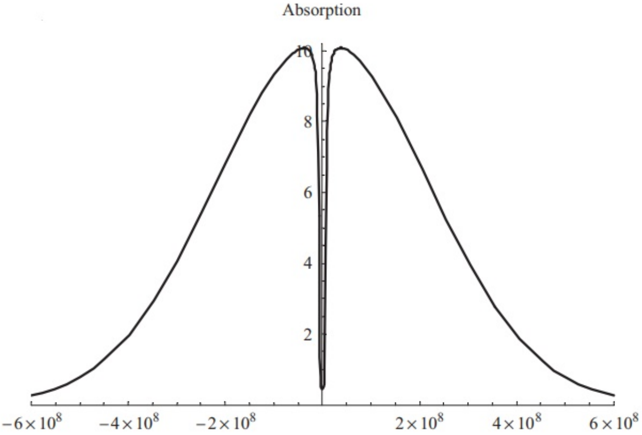

Figure 2: Theoretical results for the absorption of the probe beam. These results are obtained following a ladder-type EIT in rubidium. The $5S_{1/2} \rightarrow 5P_{3/2}$ transition serves as the probe transition at 780.2nm. The $5P_{3/2} \rightarrow 5D_{5/2}$ serves as the coupling transition at 776.0nm.

Performing EIT experimentally

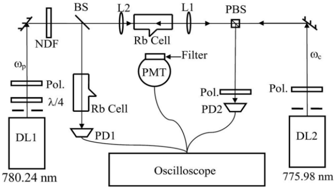

(a)

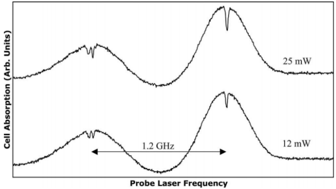

(b)

Figure 3: (a) This is the experimental setup that can be used in order to perform EIT. (b) These are results of EIT where the 1.2GHz frequency span is the window of transparency for a rubidium gas in the same configuration that was developed previously.

Modeling EIT as a mass-spring system

- If EIT is modeled properly, the expectation is that the driving force will become “transparent” to the mass for which it is driving

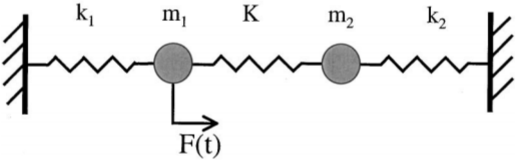

Figure 4: This is the spring mass system that will be used to model EIT.

Mathematical model

- Our goal will be to analyze the power that is transferred from the driving force to m_1

$$\ddot{x}_1 + 2\gamma_1 \dot{x}_1 + \omega_1^2 x_1 - \Omega_1^2 x_2 = \frac{F_0}{m} e^{-i\omega_s t}$$
$$\ddot{x}_2 + 2\gamma_2 \dot{x}_2 + \omega_2^2 x_2 - \Omega_2^2 x_1 = 0$$

EIT (Quantum)	Spring-mass (Classical)
Probe Field	F(t)
Coupling Field, ω_{31}	K
ω_{21}	k_1
ω_{32}	k_2
γ_{31}	γ_1
γ_2	γ_2
$\mathrm{Im}[\chi_e]$	$\mathrm{Re}[P(\omega_s)]$

Results

- We seek a solution for $x_1(t)$ and assume it in the form of $Ne^{-i\omega t}$ and assume $x_2(t)$ takes a similar form we find the solution to x_1 in the form

$$x_1(t) = \frac{F_0(\omega_2^2 - \omega_s^2 - i\gamma_2\omega_s)e^{-i\omega_s t}}{m\left[(\omega_1^2 - \omega_s^2 - i\gamma_1\omega_s)(\omega_2^2 - \omega_s^2 - i\gamma_2\omega_s) - \Omega_1^2\Omega_2^2\right]}$$

- The absorbed power from the driving force by m_1 during one period of oscillation is

$$P(\omega_s) = \frac{2\pi i F_0^2\omega_s(\omega_2^2 - \omega_s^2 - i\gamma_2\omega_s)}{m\left[(\omega_1^2 - \omega_s^2 - i\gamma_1\omega_s)(\omega_2^2 - \omega_s^2 - i\gamma_2\omega_s) - \Omega_1^2\Omega_2^2\right]}$$

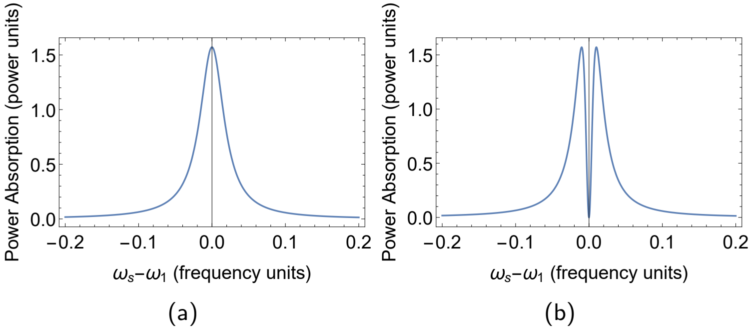

Figure 5: The values used are $m_1 = m_2 = 1.0\,\mathrm{kg}$, $\omega_1 = \omega_2 = 1.0\,\mathrm{rad/s}$, $\gamma_1 = 4.0 \times 10^{-2}$, $\gamma_2 = 1.0 \times 10^{-7}$, and $F_0 = 0.1$. The values for the coupling frequency are $\Omega_1 = \Omega_2 = \sqrt{K/m}$, and the strength of the coupling fields are (a) 0.0, (b) 0.2 in arbitrary units.

Spring-mass model under non-idealized parameters

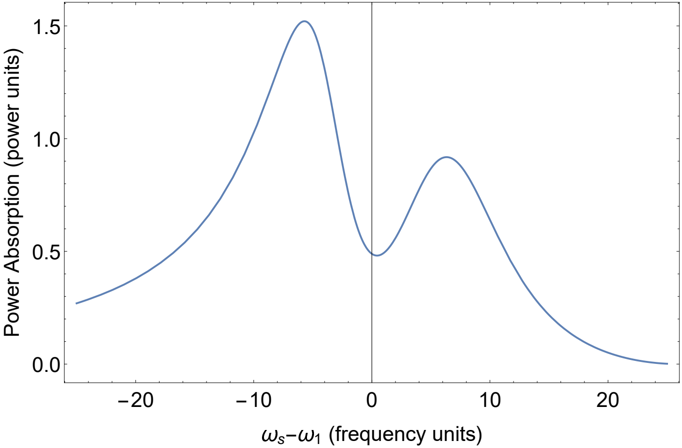

Figure 6: Theoretical graph of EIT classical analog using the following parameters, $m_1 = 0.56\,\text{kg}$, $m_2 = 0.72\,\text{kg}$, $k_1 = 415\,\text{N/m}$, $k_2 = 381\,\text{N/m}$, $K = 204\,\text{N/m}$, $\gamma_1 = 2.42$, and $\gamma_2 = 0.54$. These parameters are obtained from experiments I performed in lab using a rectilinear plant.

Spring-mass experiment

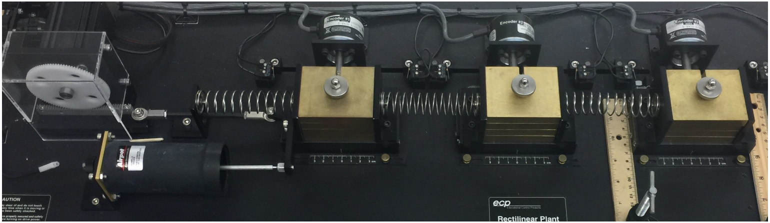

Figure 7: This is the spring mass setup I use as my classical analog to EIT with m_1 being driven by the control system (left), m_2 being coupled by the spring attached to m_1 (middle) and the right most spring is attached to a fixed wall (right most body acts as a wall).

Spring-mass experiment considerations

- Additional factors of friction to consider

$$\ddot{x}_1 + 2\gamma_1\dot{x}_1 + \omega_1^2 x_1 - \Omega_1^2 x_2 - \mu_{k1} N_1 \,\mathrm{sgn}(\dot{x}_1) = \frac{F_0}{m}\sin(\omega_s t),$$
$$\ddot{x}_2 + 2\gamma_2\dot{x}_2 + \omega_2^2 x_2 - \Omega_2^2 x_1 - \mu_{k2} N_2 \,\mathrm{sgn}(\dot{x}_2) = 0,$$

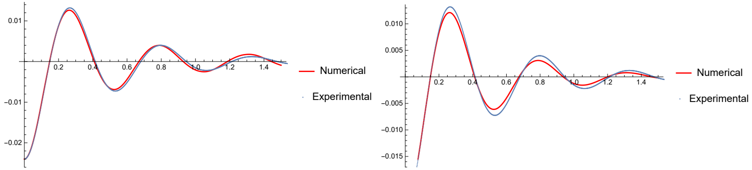

(a) (b)

Figure 8: Both figures are position v. time graphs for the first mass of the system. (a) This is the comparison of the theoretical model to data taking using the control plant, including the coulomb friction (b) without coulomb friction

Modeling EIT as a coupled RLC circuit

- If EIT is modeled properly, the expectation is that the EMF will become "transparent" to the second loop of the circuit

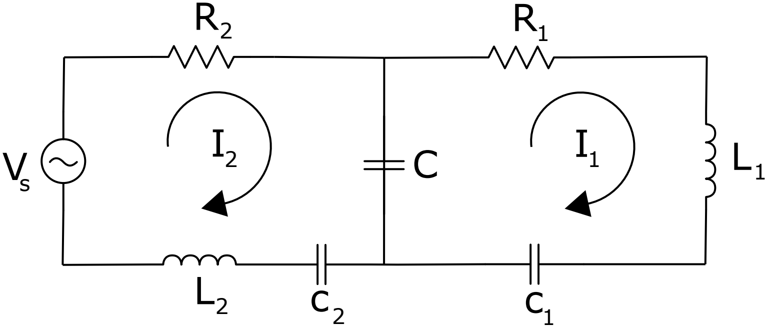

Figure 9: The electrical circuit used to study EIT-like behavior.

EIT model for circuits

- Our goal will be to analyze the power that is transferred from the AC signal V_s to $(RLC)_2$

EIT (Quantum)	RLC circuit (Classical)
Probe Field	$V_0 e^{i\omega_s t}$
Coupling Field	C
ω_{21}	$(RLC)_2$
ω_{32}	$(RLC)_1$
γ_{31}	R_1
γ_2	R_2
$\mathrm{Im}[\chi_e]$	$\mathrm{Re}[P(\omega_s)]$

Mathematical structure

$$i\,I_1 X_C + I_2\left[R_2 - i\left(X_C + X_{C_2} - X_{L_2}\right)\right] = V_s$$
$$i\,I_2 X_C + I_1\left[R_1 - i\left(X_C + X_{C_1} - X_{L_1}\right)\right] = 0$$

- From the above systems equations the current in the second loop is defined as

$$I_2 = \frac{(X_C + X_{C_1} + X_{L_1} + iR_1)(A + iB)}{A^2 + B^2} V_0$$

$$A = R_2\left(X_C + X_{C_1} - X_{L_1}\right) + R_1\left(X_C + X_{C_2} - X_{L_2}\right)$$

$$B = \left(X_{C_1} - X_{L_1}\right)\left(X_{C_2} - X_{L_2}\right) + X_C\left(X_{C_1} + X_{C_2} - X_{L_1} - X_{L_2}\right) - R_1 R_2$$

Results

$$P = \frac{(X_C + X_{C_1} + X_{L_1} + iR_1)(A + iB)}{A^2 + B^2} V_0^2$$

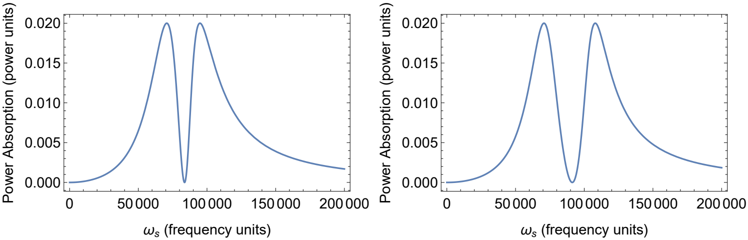

(a) (b)

Figure 10: R_1=0Ω R_1=50Ω, C_1=0.2μ F, C_2=0.2μ F, L_1=0.001 mH, L_2=0.001 mH, V_0=1.0V (a)C=0.5μ F (b)C=0.3μ F

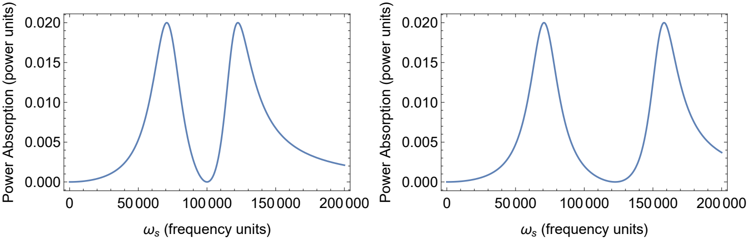

(a) (b)

Figure 11: $R_1{=}0\Omega$ $R_1{=}50\Omega$, $C_1{=}0.2\mu\,\mathrm{F}$, $C_2{=}0.2\mu\,\mathrm{F}$, $L_1{=}0.001\,\mathrm{mH}$, $L_2{=}0.001\,\mathrm{mH}$, $V_0{=}1.0V$ (a) $C{=}0.2\mu\,\mathrm{F}$ (b) $C{=}0.1\mu\,\mathrm{F}$

Coupled RLC circuit experiment

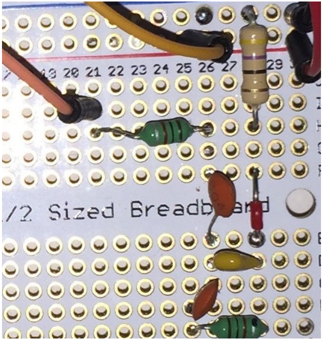

Figure 12: This is the circuit that was used to model lambda-type EIT. The orange cables are connected in order to measure the current going through the second mesh and the black and red leads supply the power to the circuit. For this experiment we used the following values, $C_1 = 0.102\mu\,\mathrm{F}$, $C_2 = 0.084\mu\,\mathrm{F}$, $C = 0.198\mu\,\mathrm{F}$, $L_1 = 0.934\,\mathrm{mH}$, $L_2 = 0.929\,\mathrm{mH}$, $R_2 = 50\Omega$ and $R_1 = 0\Omega$.

Circuit experimental results

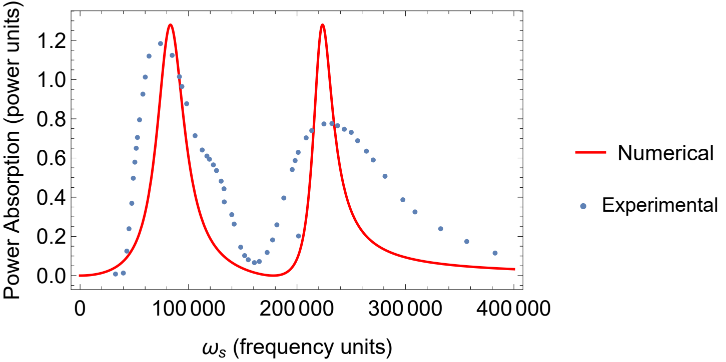

Figure 13: Comparison of the theoretical model (red) and the experimental data (dotted) using the following components: R_1=0Ω, R_1=50Ω, C_1=0.102 μF, C_2=0.084 μF, L_1=0.929 mH, L_2=0.934 mH, V_0=20.0 V, C=0.198 μF.

Conclusions

- EIT behavior can be replicated in classical systems
- The strength of the coupling fields modeled by the classical systems dictate the frequency range for which there is significant loss in absorption
- The asymmetric behavior seen is likely due to the detuning differences in the systems
- EIT as a spring mass system is unlikely to have a zero absorption window of transparency

Works Cited

[1] S. E. Harris, Physics Today (1997).
[2] L. V. Hau, S. Harris, Z. Dutton, and C. H. Behroozi, Nature , 594 (1999).
[3] Z. Bai, C. Hang, and G. Huang, Optics Communication , 253 (2013).
[4] J. R. Ackerhalt and P. W. Milonni, Phys. Rev. A **33**, 3185 (1986).
[5] A. Nazarkin, R. Netz, and R. Sauerbrey, Phys. Rev. Lett. **92**, 043002 (2004).
[6] B. S. Ham and P. R. Hemmer, Phys. Rev. Lett. **84**, 4080 (2000).
[7] P. R. Hemmer and M. G. Prentiss, J. Opt. Soc. Am. B **5**, 1613 (1988).
[8] D. B. Sullivan and J. E. Zimmerman, American Journal of Physics **39** (1971).
[9] H. Meyera, The journal of chemical physics **70** (1979).
[10] W. Frank and P. V. Brentano, American Journal of Physics **62** (1994).
[11] D.-S. Wang, Communications in Theoretical Physics **67** (2017).
[12] A. J. Olson and S. K. Mayer, American Journal of Physics **77**, 116 (2009), https://doi.org/10.1119/1.3028309.
[13] C. L. G. Alzar, M. A. G. Martinez, and P. Nussenzveig, American Journal of Physics **70**, 37 (2002).